



Original research article

Efficient hybrid image denoising scheme based on SVM classification

Sidheswar Routray^a, Arun Kumar Ray^a, Chandrabhanu Mishra^b, G. Palai^{c,*}^a School of Electronics Engineering, KIIT University, Bhubaneswar, Odisha, India^b Department of Instrumentation and Electronics, CET, Bhubaneswar, Odisha, India^c Department of Electronics and Communication, Gandhi Institute for Technological Advancement (GITA), Bhubaneswar, Odisha, India

ARTICLE INFO

Article history:

Received 12 October 2017

Accepted 20 November 2017

Keywords:

Feature extraction
Support vector machine
Patch classification
Sparse representation
Texture preservation
Image denoising

ABSTRACT

An efficient hybrid image denoising method based on support vector machine (SVM) classification is designed and developed in this communication. Here, the input noisy image is first divided into large number of overlapping patches followed by extraction of local features from each patches using scale invariant feature transform (SIFT). Based on a predefined threshold, SVM is used to classify the patches into two classes such as texture patches and flat patches. The texture patches are processed through gradient histogram preservation (GHP) where flat patches are reconstructed using sparse based denoising method using the analysis, K-SVD. Finally, the reconstructed image is obtained by merging the results of the two denoising process. To find the efficiency of our proposed hybrid denoising scheme, we perform several experiments on some standard noisy images and compare the results with some state-of-the-art denoising methods. Experiments indicate that the proposed hybrid scheme performs better denoising performance, particularly in preserving edges and textures as compared to existing denoising method.

© 2017 Elsevier GmbH. All rights reserved.

1. Introduction

Image denoising is used to estimate clean original image by removing noise from the noisy image. The main challenge of any denoising algorithm is to suppress noise while preserving texture and edge details [1]. In general, image denoising methods are classified based on their domain such as spatial-domain methods, transform-domain methods and dictionary learning based methods [2]. Spatial domain methods basically make use of correlations exist in most natural images. Broadly, spatial filters are categorized as local and nonlocal filters [3]. Some of the popular local filtering algorithms such as Gaussian filter [4], Wiener filter [5], bilateral filter [6] have been developed for noise reduction. However, for high noise level, the correlations exist between neighbouring pixels have been damaged and hence, local filters cannot perform well. Whereas, the nonlocal filters utilizes the self-similarity of natural images. Non local means (NLM) and its improvements have been developed for image denoising [7]. Nonlocal filters perform better than local filters still they have a tendency to produce artefact such as over-smoothing.

In transform-domain methods, orthonormal basis such as DCT, wavelets [8], curvelets [9], and contourlets [10] are used to represent image patches. Here, small coefficients correspond to the high-frequency part and these coefficients are correlated to image details and noise. Hence, the noise can be reduced in the reconstructed image by removing the smaller coefficients.

* Corresponding author.

E-mail addresses: gpalai28@gmail.com, g_pallai@yahoo.co.uk (G. Palai).

Some of the popular transform domain based denoising methods are BLS-GSM [11], BM3D [12], LPG-PCA [13]. Recently, sparse based image denoising has shown its popularity. The denoising is performed by learning a large group of image patches from the input noisy image in such a way that each image patch in the reconstructed image can be represented as a linear combination of a few patches in the dictionary. Some of the popular learning based image denoising methods are K-SVD [14], LSSC [15] and CSR [16]. Recently, another patch based method MS-EPLL was proposed by using Gaussian Mixed Model (GMM) to describe each clean image patch from the corresponding noisy image [34]. Also, a hybrid denoising framework was developed where different denoising methods are applied for the corresponding patches [35].

The features of an image are highly distinct and invariant to location and scale. It gives the unique information of an image. The image can be classified in to different patches based on features. Instead of applying a single filtering on all patches, we may apply different transforms on different set of patches with similar features. For example textured patches can be denoised using some texture preserved algorithm whereas flat patches can be denoised using sparse based algorithm. Unfortunately, so far there is not an explicit image denoising method based on feature based classification.

With this motivation, we develop a hybrid denoising scheme based on SVM classification. In the proposed denoising method, we first divide the noisy image into large number of overlapping patches followed by extraction of local features from each patches using SIFT. Then SVM is used to classify the patches into two classes such as texture patches and flat patches. The texture patches are processed through gradient histogram preservation (GHP) and the flat patches are reconstructed using sparse based denoising method Analysis KSVD. Finally, the reconstructed image is obtained by merging the results of the two denoising process.

The rest of the paper is planned as follows. We present the proposed image denoising framework in details in Section 2. We illustrate the experimental results in Section 3 and closing remarks are provided in Section 4.

2. Proposed image denoising framework: HYSVM

The framework for the proposed hybrid image denoising method based on support vector machine (SVM) classification HYSVM is shown in Fig. 1. In this method, we first decompose the input noisy image into large number of overlapping patches followed by extraction of the local features from each patch. To find key points in image patches, we use the most robust feature extraction method SIFT. Similar features are aggregated in to feature vectors followed by clustering. Based on a predefined threshold, the patches are classified into two classes such as texture patches and flat patches with the help of SVM. The texture patches are processed through curvelet transform and the flat patches are reconstructed using sparse based denoising method 'Analysis KSVD'. Finally, the reconstructed image is obtained by merging the results of the two denoising process. The proposed denoising scheme consists of mainly four parts such as patch classification process, texture preservation using curvelet transform, denoising of flat patches using Analysis KSVD and merging.

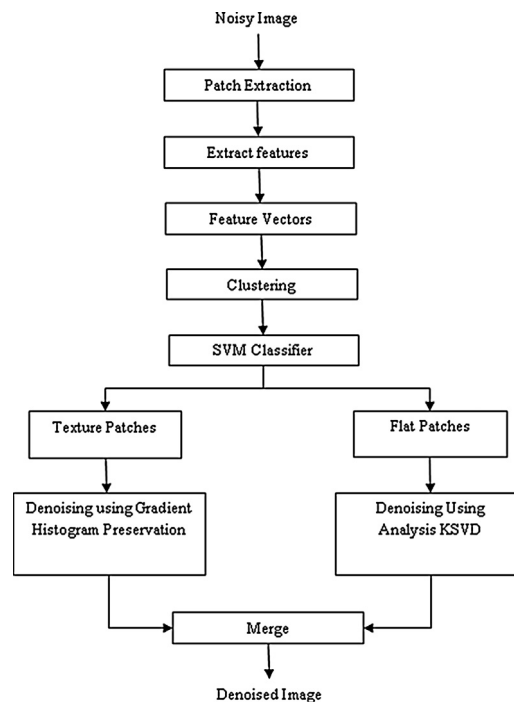


Fig. 1. Flow chart of HYSVM.

2.1. Patch classification process

We first decompose the noisy image into overlapping image patches. Using the local descriptor SIFT, we extract the distinctive invariant features of each patch. The features extracted from each image patch are grouped into N clusters of visual words using K-means. Finally, SVM classifier is used to classify patches in to two categories based on predefined threshold. The patch classification process is as follows:

2.1.1. Feature extraction using SIFT descriptor

The features of an image are highly distinct and invariant to location and scale. It gives the unique information of an image and is used for image matching. Several feature extraction methods such as SIFT, SURF and HOG are used for extraction of features from an image [17]. Here, we use SIFT to extract features and descriptors from image patches. Since SIFT extracts maximum feature points from image patch, it is preferred over other feature extraction methods [18]. SIFT provides a robust mechanism for detecting distinctive invariant image features which provide robust matching between different image patches. SIFT consist of four computational stages such as scale-space extrema detection, keypoint localization, orientation computation and keypoint descriptor [19]. Each computational stage consists of a filtering process which allows only robust keypoints to jump to next stage.

In first stage of computation, difference of gaussians (DoG) function is employed to find the keypoints [20]. The scale space of an image $L(x, y, \sigma)$ is computed by performing convolution between Gaussian function $G(x, y, \sigma)$ and the input image $I(x, y)$.

The scale space function is

$$L(x, y, \sigma) = G(x, y, \sigma) * I(x, y) \quad (1)$$

where $G(x, y, \sigma) = \frac{1}{2\pi\sigma^2} e^{-(x^2+y^2)/2\sigma^2}$

To improve the computation speed, DoG was used instead of Gaussian and is computed as

$$\begin{aligned} D(x, y, \sigma) &= (G(x, y, k\sigma) - G(x, y, \sigma)) * I(x, y) \\ &= L(x, y, k\sigma) - L(x, y, \sigma) \end{aligned} \quad (2)$$

The feature points are localized by eliminating low contrast keypoints in the second stage. In the third stage, orientations are assigned at each keypoint location based on the image gradient. The final phase measures local image gradients around each keypoint and according to keypoint orientation, descriptor orientations are rotated [21].

2.1.2. Clustering using K-means

The features extracted from each image patch in the feature extraction step are grouped into N clusters of visual words using K-means. Each extracted feature is mapped into its nearest cluster centroid using a Euclidean distance metric. Once a feature is placed in to the cluster centroid, a histogram of counts is incremented each time. As a result each patch is characterized by a histogram vector of length N . To make this process invariant to the number of features used, each histogram vector is normalised using l_2 -norm [22] (Fig 2–4).

Let the set of SIFT features is represented as $X = [x_1, \dots, x_m]^T$. The K-means clustering is applied to solve the following problem

$$\min \sum_{m=1}^M \|x_m - v_m\|^2 \quad (3)$$

where $V = [v_1, \dots, v_m]^T$ are the K cluster centres and $\|\cdot\|$ called l_2 norm.

2.2. Classification using SVM

After clustering, we introduce SVM to classify the image patches. SVM is a popular classifier scheme based on the study of supervised learning technique and is applied to classification problems [23]. In this work, we consider a SVM with a linear kernel due to its simplicity and computational efficiency in training and classification. By using a kernel function, the nonlinear samples are transformed into a high dimensional feature space where the separation of nonlinear samples or data might become possible which makes the classification convenient [24]. The SVM classifier defines a hyperplane which is used to separate two classes with a maximal margin and is represented as

$$K(x, y) = x^T y + c \quad (4)$$

where x and c are the parameters of hyperplane.

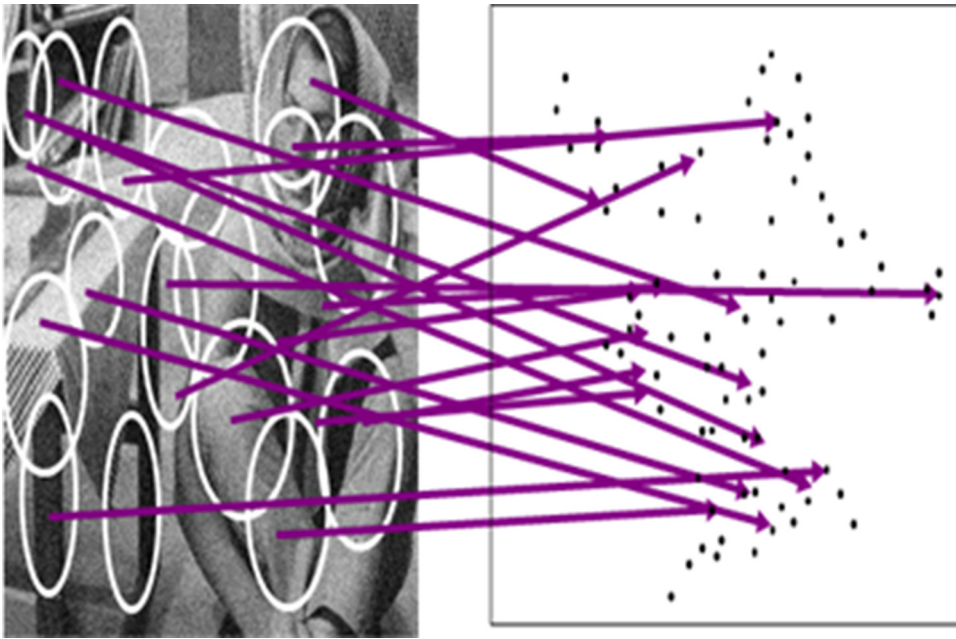


Fig. 2. Distinctive feature Points of Barbara Image.

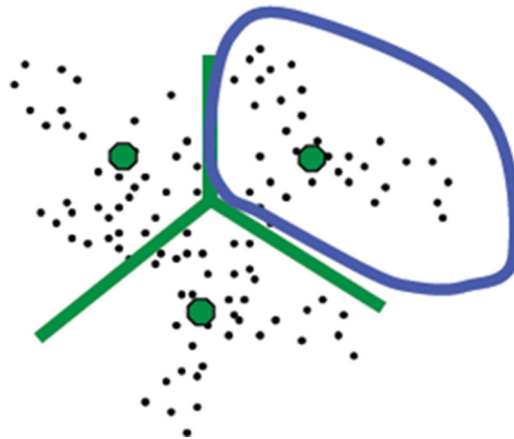


Fig. 3. Similar features of different patches are grouped into one visual word.

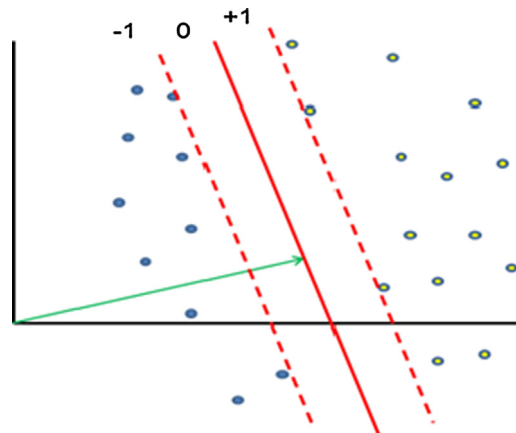


Fig. 4. SVM Classification.

Datasets are not always linear and in this case non-linear classifier is used to improve the performance. The non-linear SVM is defined in the following equation

$$K(x, y) = 1 - 2 \sum_{i=1}^n \frac{(x_i - y_i)^2}{x_i + y_i} \quad (5)$$

Here, x_i represent the training features whereas y_i represent the label of x_i . The sum is taken over selected few x_i . These feature vectors are lying nearest to the separating hyperplane and are known as support vectors [25].

2.3. Denoising of flat patches using analysis K-SVD

Image denoising using synthesis based sparse representation has shown its popularity since last decade [14]. In synthesis based sparse model, it is assumed that the signal can be represented as a linear combination of a few atoms or columns of a dictionary [26]. However, we focus on an alternative sparse based model called Analysis K-SVD for denoising of flat patches. The approach taken in Analysis K-SVD is similar to that of synthesis K-SVD [27]. However, the developments of Analysis K-SVD over synthesis K-SVD is instead of orthogonal matching pursuit (OMP), it includes the Backward Greedy algorithm. Also, it uses a penalty function for updating the dictionary [28].

Given a training set of image patches. $Y = [y_1, y_2, \dots, y_r] \in \mathbb{R}^{d \times r}$. In presence of Gaussian noise, the patch is given by $y_i = x_i + v_i$, where x_i is the noiseless image patch and v_i represents white Gaussian noise. Also, x_i satisfies a co-rank of $d - r$ with respect to the dictionary Ω . Here, the task is to find the dictionary Ω which estimates the noiseless image patch x_i . The task is formulated as

$$\{\hat{\Omega}, \hat{X}, \{\hat{\Lambda}_i\}_{i=1}^R\} = \underset{\Omega, X, \{\Lambda_i\}_{i=1}^R}{\text{Arg min}} \|X - Y\|_F^2 \quad (6)$$

$$\text{subject to } \hat{\Omega}_{\Lambda_i} x_i = 0, \forall 1 \leq i \leq R$$

$$\text{Rank}(\Omega_{\Lambda_i}) = d - r, \forall 1 \leq i \leq R$$

$$\|w_j\|_2 = 1, \forall 1 \leq j \leq p.$$

Here, x_i are the estimated noiseless patches denoted as the columns or atoms of X and Y is the set of noisy image patches corrupted by white Gaussian noise v_i . Here, $\hat{\Omega}_{\Lambda_i} x_i = 0$ indicates that the calculation of the representation is trivial, where Ω_{Λ_i} is a sub-matrix of dictionary Ω which consists of only rows indexed in Λ . Here, w_j denote the rows of Ω whereas $\|w_j\|_2$ indicates that optimization is carried out sequentially for each of the rows w_j in Ω . In dictionary update stage, only the columns of estimated image \hat{X} those are orthogonal to w_j affects the update of w_j whereas the remaining signal have no influence on w_j .

2.4. Denoising of textured patches using gradient histogram preservation

The important task of image denoising algorithm is to preserve important edge and texture details while removing noise [32]. Various denoising methods, such as nonlocal self-similarity based method, gradient based method and sparsity based method, have been widely used for noise removal. However, these methods smooth the important image structure and texture details while removing noise and hence, degrade the image visual quality [29]. Therefore, we have used a texture enhanced denoising method called gradient histogram preservation (GHP) to denoise the texture patches. GHP is used to preserve the important edge details while removing noise from noisy patches [30]. Generally, an over-smoothed image has weaker gradients as compared to the original image. Therefore, good approximation of the original image should have a similar gradient distribution to that of original image. Motivated by this fact, we apply GHP method for denoising of texture patches.

The original image x in presence of Gaussian noise v with the standard deviation σ is represented as $y = x + v$. Here, the objective is to estimate the denoised image \hat{x} from the noisy image y . Let's consider the gradient histogram of original image x and denoised image \hat{x} is denoted by h_r and h_f simultaneously. To make h_f nearly same as h_r , the GHP based image denoising method is proposed as follows [31]

$$\hat{x} = \underset{x}{\text{argmin}} \left\{ \frac{1}{2\sigma^2} \|y - x\|^2 + \lambda R(x) + \mu \|F(\nabla x) - \nabla x\|^2 \right\}, \text{ such that } h_f = h_r \quad (7)$$

Here, $R(x)$ represents the regularization term and its specific form depend on image priors, $F(\nabla x)$ denote the transformed gradient image whereas ∇ is the gradient operator. The GHP model defined in Eq. (7) is integrated with the sparsity and NSS priors and it results

$$\hat{x} = \underset{x}{\text{argmin}} \left\{ \frac{1}{2\sigma^2} \|y - x\|^2 + \lambda \sum_i \|\alpha_i - \beta_i\|_1 + \mu \|F(\nabla x) - \nabla x\|^2 \right\}, \quad (8)$$

Where α_i is the coding coefficients of x_i , β_i is the nonlocal means of α_i . Here, $x_i = R_i x$ are the patches extracted at position $i = 1, 2, 3, \dots, N$ and R_i denotes patch extraction operator and N represents number of pixels in the image. It is observed from

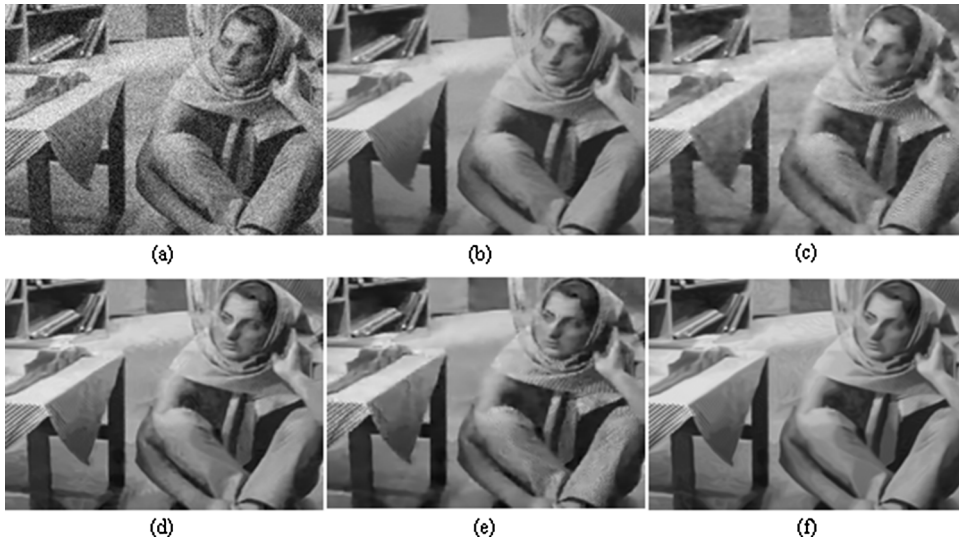


Fig. 5. Denoised Images for $\sigma = 50$ (a) Noisy Barbara Image (b) LPG-PCA (c) KSVD (d) BM3D (e) MS-EPLL (f) HYSVM.

Eq. (8) that for higher value of histogram regularization parameter λ , $F(\nabla x)$ will be close to ∇x . As a result the histogram h_F of $F(\nabla x)$ will be same as histogram $h_r x$ and it leads to the desired GHP based image denoising.

2.5. Merging

After obtaining the denoising result of flat patches with method in Section 2.3 and textured patches with method in Section 2.4, the whole image reconstructed image can be obtained by combining them.

3. Experimental results and discussion

To validate the performance of our proposed HYSVM method, we conduct the experiment on three standard images of size 256×256 such as Barbara, Lena and Cameraman. Also, we compare the proposed method with some popular denoising algorithms which include LPG-PCA [13], KSVD [14], BM3D [12] and MS-EPPL [34]. In our experiment, we set the parameters as follows. The number of patch groups K is set as 50, the patch size $l \times l$ is set as 8×8 , the parameter μ is set as 5, noise variance σ is in the range of [10,30,50,100]. The analysis dictionary $\Omega \in R^{50 \times 50}$ is generated with a data set consists of $R = 50000$ analysis signals and each signal is residing in a 4-dimensional subspace.

Peak Signal to Noise Ratio (PSNR) provides quantitative results of various denoising methods [33]. PSNR is given by

$$PSNR = 10 \log_{10} \frac{L^2}{MSE} \quad (9)$$

where L represents the highest pixel value and MSE represents the mean square error.

3.1. Qualitative and quantitative comparison

The visual quality comparison of the denoised images by all considered methods for standard deviation $\sigma = 50$ is shown in Figs. 5–7. It is observed from the experimental results that LPG-PCA, KSVD smooth much the textures, while BM3D produces some artifacts in the smooth area. However, MS-EPLL produce artifacts for high noise. However, due to the learning ability and texture preserving ability of the proposed algorithm is more robust against artifacts and also, it has better ability to preserve the edge and texture components than other competing denoising methods.

The quantitative experimental results of different image denoising algorithms are shown in Table 1. We observe that HYSVM method has better PSNR measures than LPG-PCA and KSVD for all noise levels. However, the result is inferior to BM3D for low noise level. For higher noise level, HYSVM performs better than BM3D. The proposed method has highest PSNR for image Barbara ($\sigma = 30, 100$), $\sigma = 50, 100$) and Cameraman ($\sigma = 50, 100$).

Fig. 8 shows the average PSNR value of all the considered denoising methods for different images. The average PSNR is calculated by taking the mean of PSNR for different noise levels for each image. From the figure, it is observed that our propose HYSVM method achieved highest average PSNR for all test images. BM3D attained the second highest average PSNR and provides very close PSNR values as compared to HYSVM.

It is observed from the comparison that BM3D uses fixed basis functions, which are less adaptive to the local geometry of the image whereas LPG-PCA depends on adaptive basis functions. As a result, it has better edge preserving capacity than



Fig. 6. Denoised Images for $\sigma = 50$ (a) Noisy Lena Image (b) LPG-PCA (c) KSVD (d) BM3D (e) MS-EPLL (f) HYSVM.

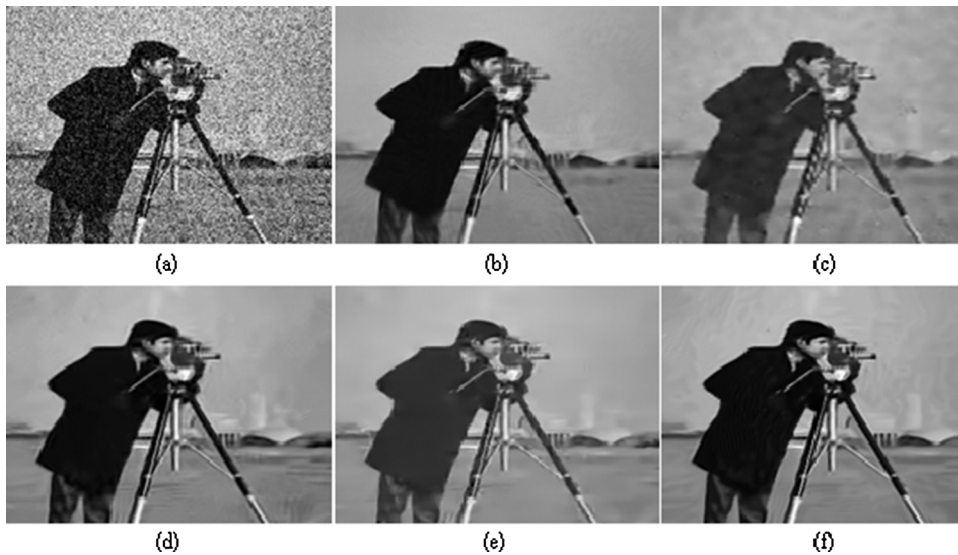


Fig. 7. Denoised Images for $\sigma = 50$ (a) Noisy Cameraman Image (b) LPG-PCA (c) KSVD (d) BM3D (e) MS-EPLL (f) HYSVM.

Table 1
PSNR (in dB) Comparison.

Image	Standard Deviation	Noisy Image	LPG-PCA	KSVD	BM3D	MS-EPLL	HYSVM
Barbara	10	28.11	33.81	34.48	34.98	33.70	34.57
	30	18.58	27.60	28.53	29.81	27.84	29.95
	50	14.17	25.00	25.45	27.23	24.99	27.98
	100	8.13	21.68	21.84	23.62	22.40	24.14
Lena	10	28.13	34.29	35.48	35.93	35.67	35.52
	30	18.59	28.35	30.43	31.26	31.19	31.13
	50	14.16	25.72	27.78	29.05	28.98	29.54
	100	8.12	22.26	24.34	25.95	26.03	26.79
Cameraman	10	28.10	33.61	33.73	34.18	34.04	33.89
	30	18.62	27.81	28.00	28.64	28.39	28.39
	50	14.13	25.43	25.65	26.12	26.12	26.73
	100	8.14	22.13	21.72	23.07	23.00	23.92

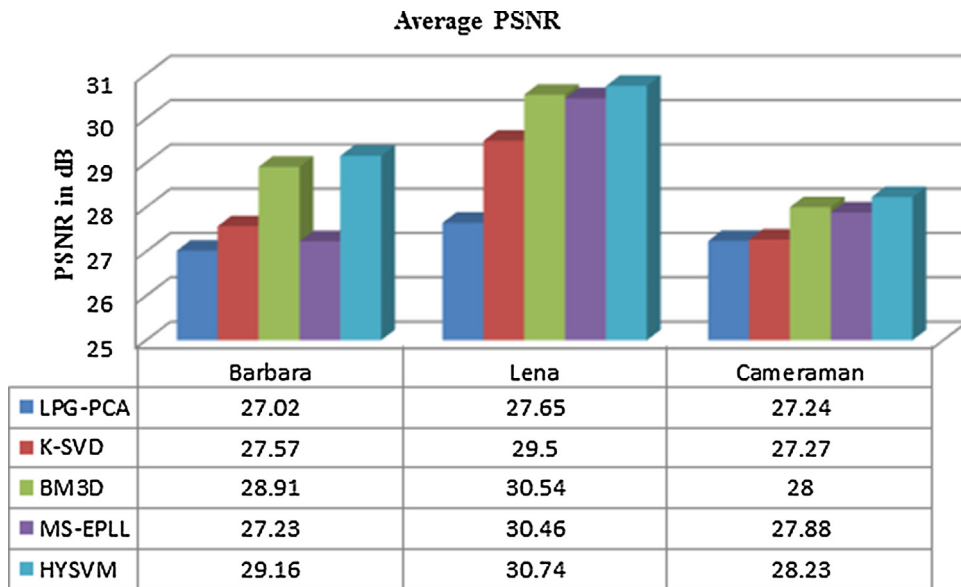


Fig. 8. Average PSNR.

Table 2

Computation time for different denoising methods (in Seconds).

Size	LPG-PCA	K-SVD	BM3D	MS-EPLL	HYSVM
256 × 256	187.2	94.08	1.02	337.05	36.39
512 × 512	748.2	80.82	5.1	1493.56	58.76

BM3D. However, in the second stage of denoising in BM3D, the noisy image patches are used to build the 3-D groups. Whereas, filtered patches are used as input of the second stage in LPG-PCA and it reduces the denoising accuracy. Since BM3D considers both overcomplete basis functions and nonlocal grouping, it performs better than other existing methods. However, K-SVD is more adaptive to natural images and shows better denoising performances by adaptive learning of a dictionary. However, the dictionary used in K-SVD needs a significant number of computations. Because of this computational load, K-SVD is not preferred for large number of patches. The major drawback of patch based approach is that image priors are imposed on intermediate results, instead of the final result. This is overcome by the introduction of MS-EPLL (Multi Scale prior Expected Patch Log Likelihood) method where the same prior is imposed on different scale patches extracted from the noisy image. However, MS-EPLL can obtain better denoising results for complex images where more details exist and is inefficient for denoising in texture and smooth areas. This is due to that the GMM prior used in MS-EPLL unable to exactly express numerous structures for the textures. In our SVM based hybrid denoising scheme, we have taken the advantages of both sparse based method Analysis K-SVD and texture preserved method GHP. Therefore, our proposed hybrid denoising scheme achieves comparable denoising performance with the BM3D or MS-EPLL.

3.2. Computational complexity

Also, we compare the computation time of all competing denoising methods. All experiments are carried out under Matlab 2014a environment on a machine with a 3.0-GHz Intel(R) 2 Core CPU. The computation time of all denoising methods for standard images of size 256×256 and 512×512 is shown in Table 2. From the table, it is seen that BM3D is the fastest method, whereas HYSVM method is the second fastest and it consumes less time than K-SVD, LPG-PCA and MS-EPLL.

4. Conclusion

This study introduced HYSVM, a hybrid based image denoising method using SVM classification. This method is basically based on feature extraction followed by classification into texture and flat patches. The texture patches are processed through gradient histogram preservation and the flat patches are reconstructed using Analysis KSVD. Finally, the reconstructed image is obtained by merging the results of the two denoising process. This method is designed to remove gaussian noise and preserve the texture information. The denoising experiments prove the efficiency of HYSVM by comparing it with some state-of-the-art denoising methods. From the result, it is observed that HYSVM provides a better denoising performance in terms of PSNR and preserves image fine structures.

References

- [1] F. Luisier, T. Blu, M. Unser, Image denoising in mixed poisson-Gaussian noise, *IEEE Trans. Image Process.* 20 (3) (2011) 696–708.
- [2] L. Shao, R. Yan, X. Li, Y. Liu, From heuristic optimization to dictionary learning: a review and comprehensive comparison of image denoising algorithms, *IEEE Trans. Cybern.* 44 (July (7)) (2014) 1001–1013.
- [3] A. Buades, B. Coll, J. Morel, 'A review of image denoising methods, with a new one', *Multiscale Model. Simul.* 4 (2) (2005) 490–530.
- [4] L. Shapiro, G. Stockman, *Computer Vision*, Prentice-Hall, Englewood Cliffs, NJ, USA, 2001.
- [5] N. Wiener, *Extrapolation, Interpolation, and Smoothing of Stationary Time Series*, Wiley, New York, NY USA, 1949.
- [6] C. Tomasi, R. Manduchi, Bilateral filtering for gray and color images, *Proc. 6th Int. Conf. Comput. Vision* (1998) 839–846.
- [7] A. Buades, B. Coll, J.M. Morel, A nonlocal algorithm for image denoising, *Proc. IEEE Int. Conf. Comput. Vision Pattern Recognit* 2 (2005) 60–65.
- [8] E.P. Simoncelli, E.H. Adelson, Noise removal via Bayesian wavelet coring, *Proc. IEEE Int. Conf. Image Process* (1996) 379–382.
- [9] J.L. Starck, E.J. Candes, D.L. Donoho, The curvelet transform for image denoising, *IEEE Trans. Image Process.* 11 (6) (2002) 670–684.
- [10] M.N. Do, M. Vetterli, The contourlet transform: an efficient directional multiresolution image representation, *IEEE Trans. Image Process.* 14 (12) (2005) 2091–2106.
- [11] J. Portilla, V. Strela, M.J. Wainwright, E.P. Simoncelli, Image denoising using scale mixtures of Gaussians in the wavelet domain, *IEEE Trans. Image Process.* 12 (11) (2003) 1338–1351.
- [12] K. Dabov, A. Foi, V. Katkovnik, K. Egiazarian, Image denoising by sparse 3-D transform-domain collaborative filtering, *IEEE Transactions Image Process.* 16 (no. 8) (2007) 2080–2095.
- [13] L. Zhang, W. Dong, D. Zhang, G. Shi, Two-stage image denoising by principal component analysis with local pixel grouping, *Pattern Recognit.* 43 (no. 4) (2010) 1531–1549.
- [14] M. Elad, M. Aharon, Image denoising via sparse and redundant representations over learned dictionaries, *IEEE Trans. Image Process.* 15 (no. 12) (2006) 3736–3745.
- [15] J. Mairal, F. Bach, J. Ponce, G. Sapiro, A. Zisserman, Non-local sparse models for image restoration, *Proc. IEEE Int. Conf. Comput. Vision* (2009) 2272–2279.
- [16] W. Dong, X. Li, L. Zhang, G. Shi, Sparsity-based image denoising via dictionary learning and structural clustering, in: *Proc. IEEE Int. Conf. Comput. Vision Pattern Recognit*, Colorado, USA, 2011, pp. 457–464.
- [17] K. Mikolajczyk, C. Schmid, Scale and affine invariant interest point detectors, *Int. J. Comput. Vision* 60 (no. 1) (2004) 63–68.
- [18] K. Mikolajczyk, C. Schmid, A performance evaluation of local descriptors, *IEEE Trans. Pattern Anal. Mach. Intell.* 27 (October (10)) (2005) 1615–1630.
- [19] D. Lowe, Distinctive image features from scale-Invariant keypoints, *IJCV* 60 (2) (2004) 91–110.
- [20] Y. Zhan-long, G. Bao-long, Image mosaic based on SIFT, *International Conference on Intelligent Information Hiding and Multimedia Signal Processing* (2008) 1422–1425.
- [21] L. Juan, O. Gwun, A comparison of SIFT, PCA-SIFT and SURF, *Int. J. Image Process.* 65 (2009) 143–152.
- [22] D. Pelleg, A. Moore, X-Means: extending K-means with efficient estimation of the number of clusters, *International Conference on Machine Learning* (2000).
- [23] S. Maji, A.C. Berg, J. Malik, Classification using intersection kernel support vector machine is efficient, *CVPR* (2008).
- [24] J. Shawe-Taylor, N. Cristianini, *Kernel Methods for Pattern Analysis*, Cambridge UK, Cambridge UP, 2004.
- [25] T. Torheim, E. Malinen, K. Kvaal, et al., Classification of dynamic contrast enhanced MR images of cervical cancers using texture analysis and support vector machines, *IEEE Trans. Med. Imaging* 33 (8) (2014) 1648–1656.
- [26] M. Elad, *Sparse and Redundant Representations: From Theory to Applications in Signal and Image Processing*, Springer-Verlag, New York NY USA, 2010.
- [27] R. Rubinstein, T. Peleg, M. Elad, Analysis K-SVD: a dictionary-learning algorithm for the analysis sparse model, *IEEE Trans. Signal Process.* 61 (3) (2013) 661–677.
- [28] W. Ruangsang, S. Aramvith, Super-Resolution for HD to 4K using analysis K-SVD dictionary and adaptive elastic-Net, in: *IEEE International Conference on Digital Signal Processing (DSP)*, Singapore, 2015, pp. 1076–1080.
- [29] T.S. Cho, C.L. Zitnick, N. Joshi, S.B. Kang, R. Szeliski, W.T. Freeman, Image restoration by matching gradient distributions, *IEEE T-PAMI* 34 (no. 4) (2012) 683–694.
- [30] W. Zuo, L. Zhang, C. Song, D. Zhang, Texture enhanced image denoising via gradient histogram preservation, in: *IEEE Conference on Computer Vision and Pattern Recognition*, Portland, OR, 2013, pp. 1203–1210.
- [31] W. Zuo, L. Zhang, C. Song, D. Zhang, H. Gao, Gradient histogram estimation and preservation for texture enhanced image denoising, *IEEE Trans. Image Process.* 23 (6) (2014) 2459–2472.
- [32] S. Routray, A.K. Ray, C. Mishra, Improving performance of K-SVD based image denoising using curvelet transform, *Proc IEEE Int. Conf. on Microwave, Optical and Communication Engineering* (2015) 381–384.
- [33] Z. Wang, A.C. Bovik, H.R. Sheikh, E.P. Simoncelli, Image quality assessment: from error visibility to structural similarity, *IEEE Trans. Image Process.* 13 (April (4)) (2004) 600–612.
- [34] V. Pappayan, M. Elad, Multi-scale patch-based image restoration, *IEEE Trans. Image Process.* 25 (January (1)) (2016) 249–261.
- [35] Y. Chen, Y. Tang, L. Zhou, A. Jiang, N. Xu, Hybrid framework for image denoising with patch prior estimation, in: *IEEE International Conference on Digital Signal Processing (DSP)*, Beijing, 2016, pp. 447–451.